# Use of terbium as a probe of tRNA tertiary structure and folding

M. R. Hargittai and K. Musier-Forsyth

*RNA* 2000 6: 1672-1680

*RNA* (2000), *6*:1672–1680. Cambridge University Press. Printed in the USA.


**METHOD**

# Use of terbium as a probe of tRNA tertiary structure and folding

**MICHELE R. SEFFERNICK HARGITTAI[1] and KARIN MUSIER-FORSYTH[1,2]**

[1]Department of Biochemistry, Molecular Biology, and Biophysics, University of Minnesota Medical School, Minneapolis, Minnesota 55455, USA
[2]Department of Chemistry, University of Minnesota, Minneapolis, Minnesota 55455, USA

## ABSTRACT

**Lanthanide metals such as terbium have previously been shown to be useful for mapping metal-binding sites in RNA. Terbium binds to the same sites on RNA as magnesium, however, with a much higher affinity. Thus, low concentrations of terbium ions can easily displace magnesium and promote phosphodiester backbone scission. At higher concentrations, terbium cleaves RNA in a sequence-independent manner, with a preference for single-stranded, non-Watson–Crick base-paired regions. Here, we show that terbium is a sensitive probe of human $tRNA^{Lys,3}$ tertiary structure and folding. When 1 $\mu$M tRNA is used, the optimal terbium ion concentration for detecting $Mg^{2+}$-induced tertiary structural changes is 50–60 $\mu$M. Using these concentrations of RNA and terbium, a magnesium-dependent folding transition with a midpoint ($K_{Mg}$) of 2.6 mM is observed for unmodified human $tRNA^{Lys,3}$. At lower $Tb^{3+}$ concentrations, cleavage is restricted to nucleotides that constitute specific metal-binding pockets. This small chemical probe should also be useful for detecting protein induced structural changes in RNA.**

**Keywords: lanthanides; magnesium; metal binding; RNA cleavage; $tRNA^{Lys,3}$**

## INTRODUCTION

The lanthanide metals have been widely used to map metal-binding sites in RNA (Ciesiolka et al., 1989a, 1989b; Marciniec et al., 1989; Gast et al., 1996; Michalowski et al., 1996; Dorner & Barta, 1999). The binding constants for lanthanide metals have been reported to be 600- to 10,000-fold higher than those for magnesium (Kayne & Cohn, 1974; Wolfson & Kearns, 1975; Draper, 1985). Thus, low concentrations of lanthanide metals easily displace magnesium. Once bound to RNA, lanthanides cleave the phosphodiester backbone by abstracting a hydrogen ion from the 2′-hydroxyl of a nearby nucleotide (Ciesiolka et al., 1989a; Matsumura & Komiyama, 1997). The 2′-oxyanion attacks the adjacent phosphodiester bond, resulting in backbone scission. Although most metals in the lanthanide series can induce RNA cleavage (Ciesiolka et al., 1989a; Komiyama et al., 1992), europium and terbium have been the most extensively studied, in part, due to their additional luminescent properties (Horrocks, 1993).

Reprint requests to: Karin Musier-Forsyth, University of Minnesota, Department of Chemistry, 207 Pleasant Street S.E., Minneapolis, Minnesota 55455, USA; e-mail: musier@chem.umn.edu.

Lanthanide ions have also been developed for use in a wide variety of biotechnological applications. For example, chelated lanthanide ion complexes have been covalently attached to antisense oligonucleotides designed to anneal to a target RNA to generate site-specific cleavage (Morrow et al., 1992; Hall et al., 1994, 1996; Magda et al., 1994; Komiyama, 1995; Baker et al., 1999). The lanthanide metals cerium and lanthanum and their complexes have also been used to cleave DNA (Takasaki & Chin, 1994; Komiyama, 1995; Branum & Que, 1999).

Although lanthanide cleavage studies of RNA have been largely limited to mapping metal-binding sites, Walter et al. (2000) recently reported the use of terbium to detect secondary and tertiary structural features of the hairpin ribozyme. When low concentrations of terbium were used (40–100 $\mu$M), cleavage only occurred at high-affinity metal-binding sites. However, at higher terbium:RNA ratios, the terbium cleaved not only the metal-binding pockets, but also non-Watson–Crick base-paired and single-stranded regions of the RNA. These researchers concluded that terbium is a versatile probe of RNA structure (Walter et al., 2000).

We were interested in characterizing the sensitivity of the terbium cleavage assay on the tertiary structure

of human $tRNA^{Lys,3}$. HIV-1 reverse transcriptase uses this tRNA as a primer to initiate retroviral reverse transcription (Wain-Hobson et al., 1985; Rhim et al., 1991; Das et al., 1994; Coffin et al., 1997). The 3′ 18 nt of human $tRNA^{Lys,3}$ are perfectly complementary to the genomic RNA primer binding site. Prior to initiation of reverse transcription, a binary complex forms between these two RNAs that involves major conformational changes in the tertiary structure of both nucleic acids (Isel et al., 1995; Skripkin et al., 1996). In vitro, the HIV-1 nucleocapsid protein (NC) facilitates the annealing of $tRNA^{Lys,3}$ to the primer-binding site (Barat et al., 1989; Darlix et al., 1995). Acceptor stem strand separation is a prerequisite to primer annealing. However, using fluorescence resonance energy transfer, we recently determined that the acceptor stem of $tRNA^{Lys,3}$ does *not* separate upon NC binding in the absence of the RNA genome (Chan et al., 1999), a result that is consistent with recent NMR data (C. Tisné, B.P. Roques, and F. Dardel, submitted). The fluorescence data could not determine whether NC induces other structural changes upon tRNA binding, such as partial or complete tertiary structure unfolding. To address this question, we wanted to develop a chemical probing method that would allow us to measure more subtle tRNA structural changes upon protein binding.

Lead has been extensively employed as a useful probe of tRNA tertiary structure. For example, yeast $tRNA^{Phe}$ possesses a high affinity lead-binding site that results in specific D-loop cleavage (Sundaralingam et al., 1984; Brown et al., 1985; Ciesiolka et al., 1989a; Marciniec et al., 1989; Khan et al., 1996; Michalowski et al., 1996). However, based on the known crystal structures of lead (Rubin & Sundaralingam, 1983; Sundaralin gam et al., 1984; Brown et al., 1985), magnesium (Holbrook et al., 1977; Hingerty et al., 1978; Quigley et al., 1978), and the lanthanide metal samarium (Robertus et al., 1974; Stout et al., 1978) bound to yeast $tRNA^{Phe}$, as well as tRNA cleavage studies conducted with all three metals (Ciesiolka et al., 1989a; Marciniec et al., 1989; Michalowski et al., 1996), trivalent lanthanides mimic magnesium ion binding more closely than lead. Moreover, lanthanide ion cleavage appears to be more general and versatile than lead cleavage (Ciesiolka et al., 1989a, 1989b; Marciniec et al., 1989; Michalowski et al., 1996; Walter et al., 2000). Specific lead cleavage of yeast $tRNA^{Phe}$ is inhibited upon NC binding (Khan et al., 1996), suggesting that NC does alter the tRNA tertiary structure. We find that the terbium cleavage pattern of human $tRNA^{Lys,3}$ is also altered upon NC binding (M.R.S. Hargittai & K. Musier-Forsyth, in prep.). To assist in the interpretation of these NC-induced changes, which will be reported in a separate manuscript, we characterized the terbium cleavage pattern of human $tRNA^{Lys,3}$ as a function of terbium and magnesium ion concentration. We find that in addition to its well-known capability to identify magnesium-binding sites in RNA, terbium is a sensitive probe of tRNA tertiary structure and folding.

## RESULTS AND DISCUSSION

### Effect of terbium ion concentration on the cleavage pattern of unfolded and folded $tRNA^{Lys,3}$

We first determined the sensitivity of human $tRNA^{Lys,3}$ to different terbium cleavage conditions. A terbium titration was performed using both "unfolded" (0 mM $Mg^{2+}$) and folded (10 mM $Mg^{2+}$) $tRNA^{Lys,3}$. Throughout this work we designate the tRNA prepared in the absence of magnesium as "unfolded," even though this molecule has substantial secondary structure and possibly weak tertiary interactions as well (Maglott et al., 1998). Our initial goal was to obtain the optimal terbium:RNA ratio for detecting structural features in the tRNA. Using 1 $\mu$M tRNA, we varied the terbium concentration over the range of 0 to 5 mM and the results are shown in Figure 1. At low terbium concentrations (0.03 mM), both the unfolded and the folded tRNAs are weakly cleaved at only a few positions. Cleavage is observed primarily at nt 15, 16, and 36. In most cases, cleavages are stronger in the folded than the unfolded tRNA. At 0.05 mM terbium, the unfolded tRNA was cleaved at nearly every position (Fig. 1). This cleavage pattern remained fairly constant up to 0.1 mM terbium. At terbium concentrations greater than 0.1 mM, weak protection from cleavage was observed in the unfolded RNA at nt 12–14 and 22–24, presumably due to some terbium-induced structural perturbations.

At terbium concentrations greater than 0.04 mM, the pattern of cleavage observed for the folded tRNA was remarkably different than that of the unfolded tRNA. In the folded tRNA, the A-form helical regions are protected from cleavage when compared to the unfolded tRNA cleaved at the same terbium concentration. Differences in the extent of cleavage for the folded tRNA revealed significant protection from cleavage in the 0.05–0.06 mM terbium concentration range, with the exception of position 15, where enhanced cleavage is observed (Fig. 1). Between 0.07 and 0.1 mM terbium, protection was slightly less evident at most positions of the folded tRNA. Above 0.1 mM terbium, increased protection from terbium cleavage is once again observed. At these higher terbium concentrations, the terbium appears to slightly alter the tRNA tertiary structure, as also observed in the unfolded molecule. Terbium has been reported to support DNA structure at high concentration by binding to the phosphodiester backbone (Tajmir-Riahi et al., 1993). Based on these observations, the optimal terbium concentration range for detecting magnesium-dependent tertiary structural features of 1 $\mu$M tRNA is 0.05–0.06 mM.

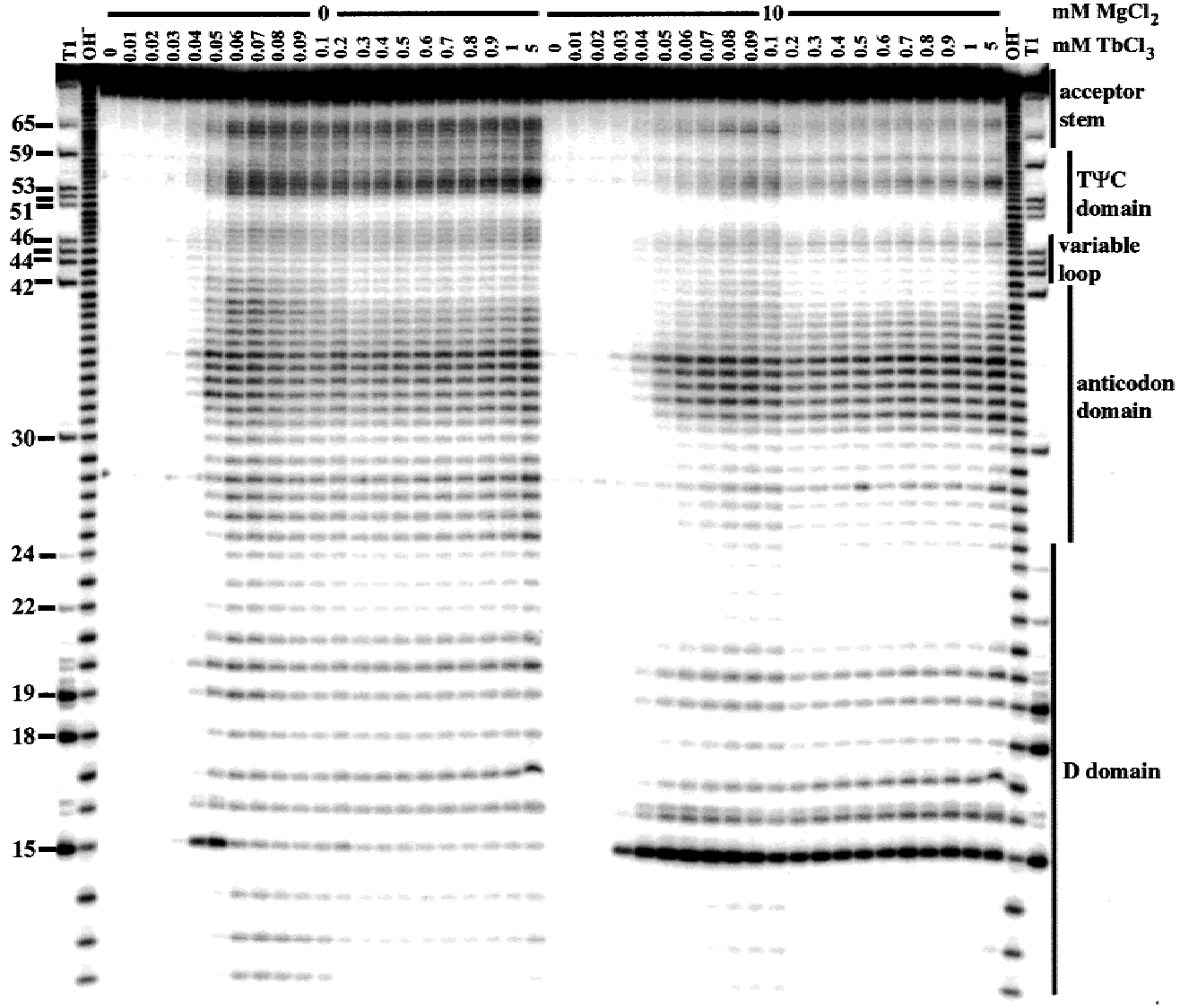


**FIGURE 1.** Phosphorimage showing the results of terbium-induced cleavage of unfolded (0 mM $Mg^{2+}$) and folded (10 mM $Mg^{2+}$) $tRNA^{Lys,3}$ at varying terbium concentrations. 5′-[$^{32}$P]-end-labeled $tRNA^{Lys,3}$ was incubated with the concentration of terbium indicated above each lane. Lanes labeled T1 correspond to tRNA digested with RNase T1, and lanes labeled $OH^-$ correspond to a partial alkaline hydrolysis ladder. The tRNA nucleotide position is indicated on the left side of the gel and the corresponding tRNA domain is indicated on the right.

One of the most striking features in the terbium cleavage pattern is the strong cleavage at position 15 in the folded tRNA. Terbium is known to have a high affinity for magnesium-binding sites in RNA (Wolfson & Kearns, 1975; Draper, 1985) and can readily displace the magnesium and induce cleavage (Ciesiolka et al., 1989a, 1989b; Marciniec et al., 1989; Gast et al., 1996; Michalowski et al., 1996). In $tRNA^{Lys,3}$, position 15 is especially sensitive to cleavage when folded. However, when the metal-binding site is not formed prior to the addition of terbium, as in the unfolded tRNA, enhanced cleavage is generally not present at position 15. At low (0.04 and 0.05 mM) terbium concentrations, the unfolded tRNA does exhibit enhanced cleavage at position 15. Since the metal-binding site is presumably not formed prior to the addition of terbium, a terbium ion may assist in the formation of the binding pocket. At low terbium concentrations, this apparently occurs before inducing more random cleavage at other sites, resulting in stronger cleavage at position 15. At higher concentrations of terbium ($\geq$0.06 mM), the metal-binding pocket is not evident in the unfolded tRNA, and position 15 is cleaved to a similar extent as the surrounding nucleotides (Fig. 1).

In Figure 2, the percent cleavage at 0.05 mM terbium for the folded and unfolded tRNAs is plotted as a function of the nucleotide positions for which quantitative data could be obtained. The most prominent cleavage events in the folded tRNA were proximal to nt 15 and

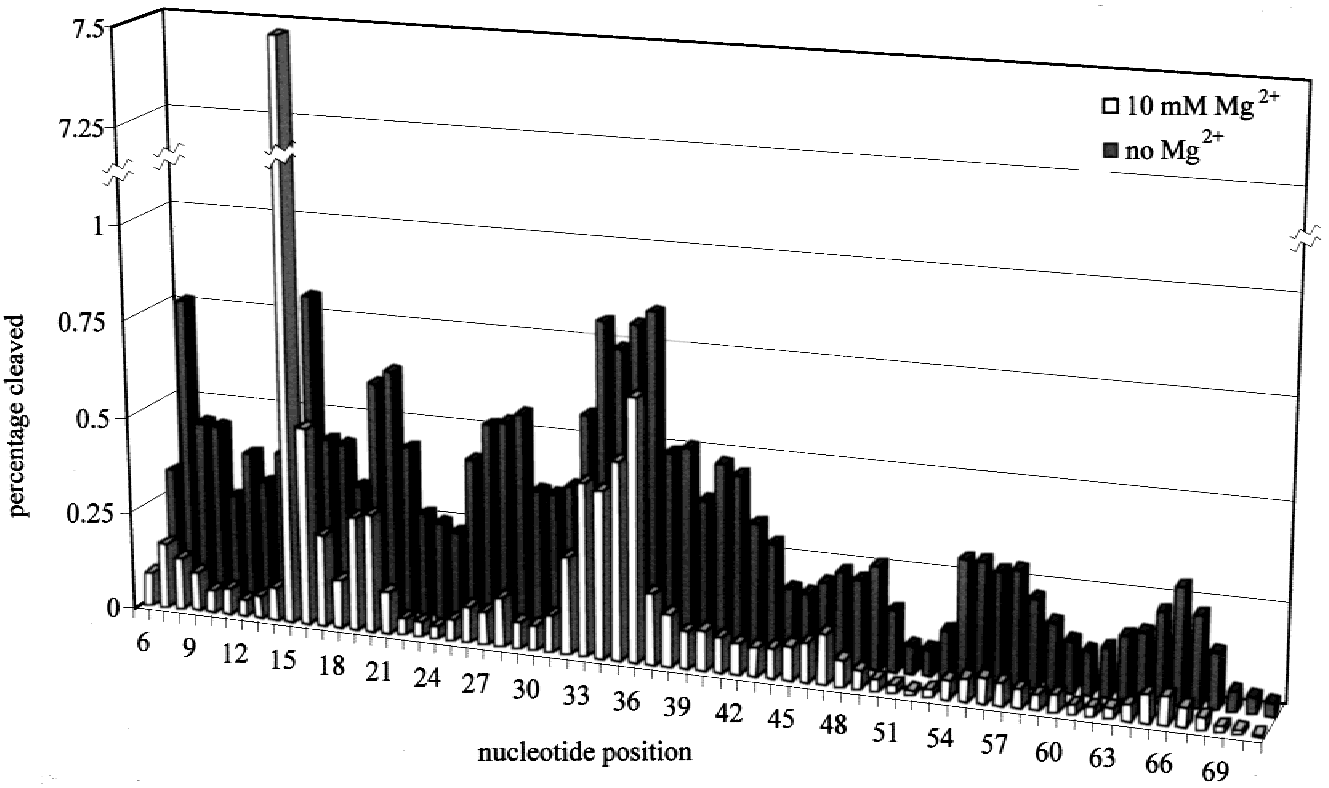


**FIGURE 2.** Bar graph showing relative percent cleavage at each nucleotide position of the unfolded (filled bars) and folded (open bars) tRNA incubated with 0.05 mM terbium. The graph shows the average percent cleavage at each position based on quantitation of 5–10 separate experiments. The percent cleavage was calculated by subtracting the background volume (at 0 mM terbium and the appropriate concentration of magnesium), dividing by the total activity in each lane (sum of the background subtracted volumes for cleavage at positions 6–76), and multiplying by 100%.

36. This graph shows that the helical regions are largely protected from cleavage in the folded tRNA. In particular, strong protection (≥70% relative to unfolded tRNA) from cleavage is observed at nucleotide positions 6–14, 21–31, 28–43, 48–59, 61–64, and 66–71.

The cleavage results obtained at 0.05 mM terbium, in the presence and absence of 10 mM magnesium, are also indicated on the L-shaped tRNA shown in Figure 3A. Cleavage was observed throughout the tRNA sequence in the unfolded state (Fig. 3A, left). Upon folding the tRNA in the presence of magnesium, the helical regions are protected from cleavage and the primary sites of cleavage (black, blue, and green balls) are in the anticodon loop and the tertiary core (Fig. 3A, right). These domains constitute well-known metal-binding pockets in tRNA (Holbrook et al., 1977; Quigley et al., 1978; Sundaralingam et al., 1984; Ciesiolka et al., 1989a, 1989b; Marciniec et al., 1989; Michalowski et al., 1996). The cleavage observed in the folded tRNA is also mapped onto the secondary cloverleaf structure of $tRNA^{Lys,3}$ shown in Figure 3B. This figure also shows that cleavage by terbium does not appear to be sequence specific.

These cleavage experiments are consistent with the presence of three to four high-affinity terbium-binding pockets in $tRNA^{Lys,3}$ (Figs. 2 and 3). This number is in good agreement with X-ray crystallography (Robertus et al., 1974; Stout et al., 1978), europium and terbium luminescence (Kayne & Cohn, 1974; Wolfson & Kearns, 1975; Draper, 1985), NMR (Jones & Kearns, 1974), and theoretical studies (Misra & Draper, 2000) carried out with other tRNAs. The D-loop contains at least two terbium-binding pockets. One terbium is located near position 15, where the strongest cleavage is observed in the folded tRNA. This terbium ion is also likely to be responsible for the modest cleavage observed at positions 16 and 17 and weak cleavage at position 18. A second terbium-binding site is located near the 3′ end of the D-loop where modest cleavage is observed at positions 19 and 20, with weaker cleavage at position 47. A third terbium-binding site is likely to be located near positions 7 and 8, which are both weakly cleaved. The anticodon-loop contains a fourth terbium-binding site. Cleavage extends from position 32 to 37, with the strongest cleavage at position 36. These four terbium-binding sites mapped by terbium cleavage of $tRNA^{Lys,3}$ correspond to the approximate location of magnesium-binding sites as determined from the X-ray crystal structure of yeast $tRNA^{Phe}$ (Fig. 3A, open circles) (Holbrook et al., 1977; Hingerty et al., 1978; Quigley et al., 1978).

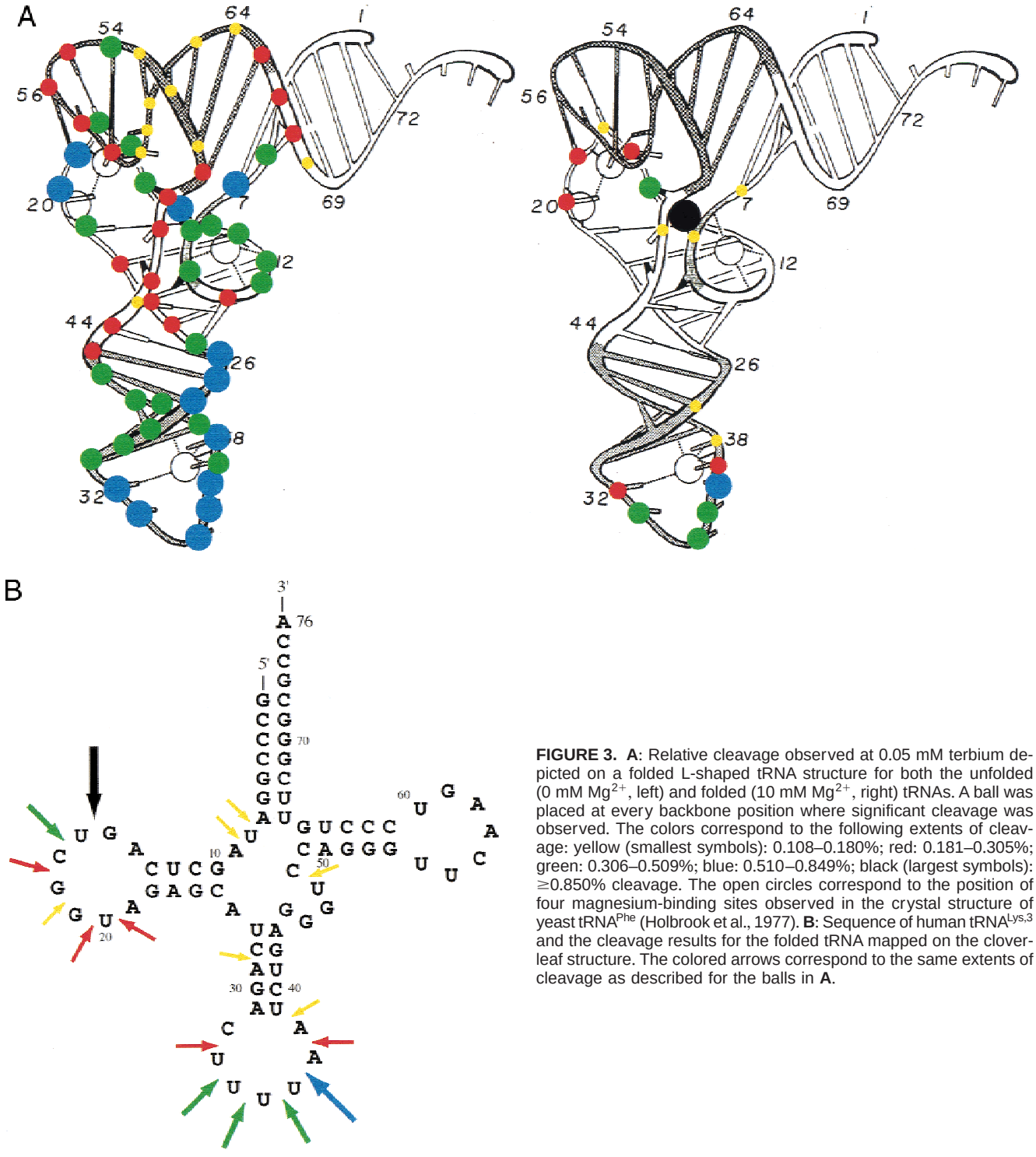


**FIGURE 3.** **A**: Relative cleavage observed at 0.05 mM terbium depicted on a folded L-shaped tRNA structure for both the unfolded (0 mM $Mg^{2+}$, left) and folded (10 mM $Mg^{2+}$, right) tRNAs. A ball was placed at every backbone position where significant cleavage was observed. The colors correspond to the following extents of cleavage: yellow (smallest symbols): 0.108–0.180%; red: 0.181–0.305%; green: 0.306–0.509%; blue: 0.510–0.849%; black (largest symbols): ≥0.850% cleavage. The open circles correspond to the position of four magnesium-binding sites observed in the crystal structure of yeast $tRNA^{Phe}$ (Holbrook et al., 1977). **B**: Sequence of human $tRNA^{Lys,3}$ and the cleavage results for the folded tRNA mapped on the cloverleaf structure. The colored arrows correspond to the same extents of cleavage as described for the balls in **A**.

Magnesium competition assays have also concluded that the lanthanide metal europium binds to the same sites on tRNA as magnesium (Wolfson & Kearns, 1975; Draper, 1985; Gast et al., 1996). This assay does not measure the binding affinities of each bound metal. Since cleavage is dependent on terbium's accessibility to the 2′-hydroxyl, the strength of the cleavage depends on the distance between the terbium and the 2′-hydroxyl of the nucleotides comprising the binding pocket.

### Sensitivity of terbium cleavage pattern of $tRNA^{Lys,3}$ to magnesium ion concentration

The previous experiments established that terbium is indeed a good probe of the folded state of tRNA. We next

wished to ask the question: Is terbium cleavage sensitive enough to detect conformational changes as the tRNA folds to a stable tertiary structure? To address this question, terbium cleavage was monitored as a function of magnesium concentration. Based on the results obtained in the presence and absence of 10 mM magnesium (Fig. 1), cleavage was performed over a range of magnesium concentrations using 0.03 mM, 0.05 mM, and 0.07 mM terbium. At each terbium concentration, the magnesium concentration was increased in 1 mM increments from 0 to 10 mM. As expected, the lowest concentration of terbium employed (0.03 mM) only cleaved sites proximal to the terbium-binding pockets (Fig. 4, lanes 3–11). At the higher terbium concentrations, in the absence of magnesium, the tRNA was cleaved at virtually every position (Fig. 4, lanes 12 and 21). Of the two higher terbium concentrations used in this experiment, 0.05 mM appeared more sensitive to magnesium-induced folding transitions in $tRNA^{Lys,3}$ than 0.07 mM. Even upon addition of only 1 mM magnesium, significant changes in the 0.05 mM terbium cleavage pattern were observed. For example, nt 12–14, 21–30, and 51–53 are protected from cleavage, whereas cleavage is enhanced at nt 15. These protected regions are primarily located in the D and anticodon stems. As the magnesium concentration is increased further, cleavage in the helical regions continues to decrease and additional regions of protection are observed. We also observe a direct correlation between the magnesium concentration and the increased intensity of cleavage at nt 15. We presume that as the magnesium concentration increases, the metal-binding pocket within the D-loop becomes more well defined. As this occurs, terbium's affinity for this site also increases and the lanthanide ion can more readily enter the metal-binding site, displace magnesium, and induce cleavage at nt 15. A much less dramatic increase in cleavage was also observed at neighboring nt 16.

The accessibility of tRNA nucleotides at positions 58, 59, and 60 to cleaving agents has previously been used as an indicator of tRNA folding because these nucleotides participate in tertiary interactions within the highly structured tRNA core (Latham & Cech, 1989; Ramesh et al., 1997; Shelton et al., 1999). For example, in unfolded yeast $tRNA^{Phe}$, positions 58, 59, and 60 are highly susceptible to cleavage by hydroxyl radicals (Latham & Cech, 1989; Ramesh et al., 1997). Upon tertiary structure formation, these positions are buried in the tRNA tertiary structure, thereby being protected from hydroxyl radical attack. Thus, cleavage at these positions can be used to monitor the extent of tRNA folding. The plot shown in Figure 5 indicates that the extent of terbium cleavage at positions 58, 59, and 60 does indeed vary as a function of the magnesium ion concentration. A magnesium-dependent transition is observed with a midpoint ($K_{Mg}$) value of 2.58 ± 0.09 mM (Fig. 5). These data also indicate that folding is essentially complete at a concentration of 6 mM magnesium, in general agreement with values reported for unmodified yeast $tRNA^{Phe}$ (Friederich & Hagerman, 1997; Maglott et al., 1998).

## CONCLUDING REMARKS

In addition to its well-established capability to map metal-binding sites in RNA, we have shown that terbium is a sensitive probe of tRNA structure and folding. Using 1 $\mu$M tRNA, we find that the optimal concentration of terbium to detect tRNA structural changes is 50–60 $\mu$M. Under these conditions, we detected a magnesium-dependent transition with a midpoint of 2.6 mM magnesium. Although human $tRNA^{Lys,3}$ is the only RNA examined by this technique to date, we imagine that this will be a useful probe for monitoring folding in other RNAs (Walter et al., 2000). The terbium ion concentration may have to be optimized for each system to maximize its sensitivity to folding. The small size of this chemical probe and its relative ease of use should not only make it a useful reagent for probing a wide variety of RNA structures, but also for detecting protein induced conformational changes in RNA tertiary structure and folding.

## MATERIALS AND METHODS

### RNA preparation

Unmodified human $tRNA^{Lys,3}$ was prepared by in vitro transcription (Milligan et al., 1987) of the *Fok*I digested pK-F119, a plasmid containing the gene for human $tRNA^{Lys,3}$ located downstream from a T7 RNA polymerase promoter (Chan & Musier-Forsyth, 1997). RNA with a free 5′-OH was transcribed by addition of 4 mM guanosine and 1 mM of each of the NTPs to the transcription reaction. The transcripts were gel purified on an 8% denaturing polyacrylamide gel. The 5′-OH-containing $tRNA^{Lys,3}$ was radiolabeled with $\gamma$-[$^{32}$P]-ATP and polynucleotide kinase. After gel purification, the radiolabeled tRNA was dissolved in diethyl pyrocarbonate-treated water and stored at −20 °C.

Prior to use, the tRNA was refolded in 50 mM HEPES, pH 7.5, and 20 mM NaCl by heating at 80 °C for 2 min then cooling to 60 °C for 2 min, followed by addition of $MgCl_2$ to 10 mM and placing on ice. The unfolded tRNA was prepared in 50 mM HEPES, pH 7.5, and 20 mM NaCl by heating at 80 °C for 2 min then placing on ice.

### $TbCl_3$ cleavage assays

The highest purity terbium (99.999%), purchased from Sigma, was freshly dissolved in diethyl pyrocarbonate-treated water daily. The refolded or unfolded tRNA (1.25 $\mu$M final concentration) was added to a solution containing 62.5 mM HEPES, pH 7.5, 25 mM NaCl, and 0–12.5 mM $MgCl_2$. To initiate the cleavage reaction, an 8-$\mu$L aliquot of this mixture was combined with 2 $\mu$L of an appropriate dilution of $TbCl_3$ to achieve a final $Tb^{3+}$ concentration of 0 to 5 mM. Thus, the final reaction mixture contained 50 mM HEPES, pH 7.5, 20 mM

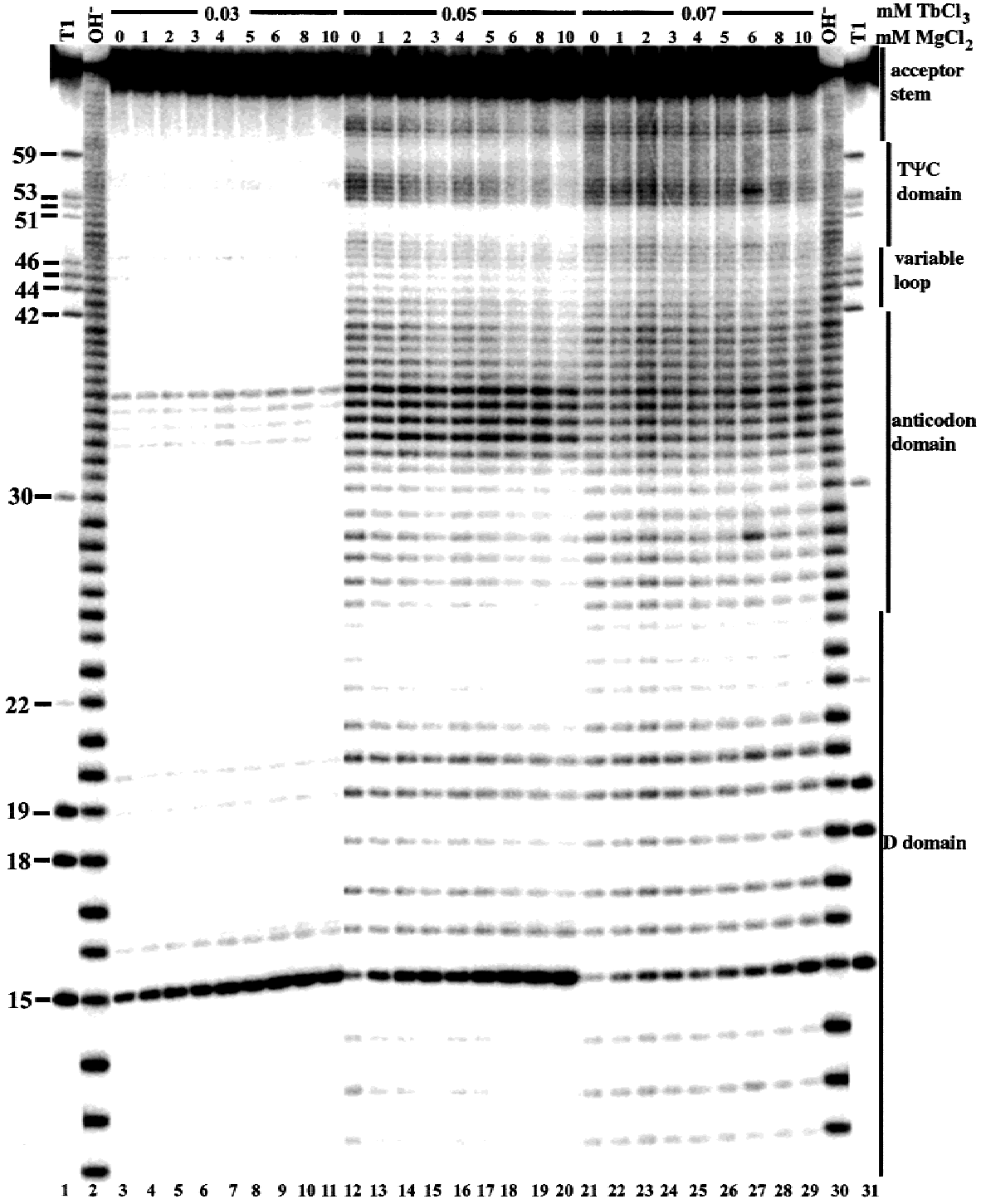


**FIGURE 4.** Terbium-induced cleavage of $tRNA^{Lys,3}$ as a function of magnesium concentration. The 5′-[$^{32}$P]-end-labeled tRNA was incubated at the magnesium concentration indicated at the top of the gel and cleaved with 0.03 mM (lanes 3–11), 0.05 mM (lanes 12–20), or 0.07 mM (lanes 21–29) terbium. Lanes labeled T1 and $OH^-$ are as described in the legend to Figure 1.

NaCl, 0–10 mM $MgCl_2$, 1 $\mu$M [$^{32}$P]-tRNA ($5 \times 10^4$ cpm), and 0–5 mM $TbCl_3$. The reaction was incubated at 37 °C for 15 min and quenched by adding EDTA, pH 8.0, to a final concentration of 45 mM and placing on ice. The tRNA was ethanol precipitated at −20 °C and redissolved in 10 mM Tris-HCl, pH 7.5, 1 mM EDTA.

An alkaline hydrolysis cleavage ladder was generated by incubating the tRNA in 50 mM sodium carbonate and 3 mM EDTA, pH 8.0, at 90 °C for 5 min. The samples were placed on ice to quench the cleavage reaction. The RNase T1 digest was performed by incubating the tRNA, 13 mM sodium citrate, and 4.6 mM EDTA, pH 8.0, at 80 °C for 2 min then

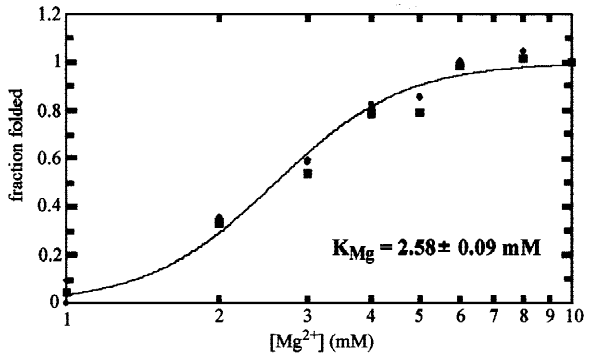


**FIGURE 5.** Graph showing magnesium-dependent folding transition based on cleavage observed at 0.05 mM terbium. The percent cleavage at positions 58 (♦), 59 (●), and 60 (■) was used to generate this plot. The percent cleavage was converted to fraction folded by normalizing each set of data from 0 (0 mM $Mg^{2+}$) to 1.0 (10 mM $Mg^{2+}$). The fit that is shown is for the data observed using cleavage at position 59. The magnesium concentration at the midpoint of the folding transition, $K_{Mg}$, was calculated as described previously (Shelton et al., 1999).

cooling to 50 °C. Cleavage was initiated upon addition of 100 mU RNase T1 from USB. The samples were incubated at 50 °C for 15 min then placed on ice. Prior to analysis by gel electrophoresis, an equal volume of 100% formamide was added to all samples, which were then denatured at 80 °C for 3 min and placed on ice. The cleavage products were separated on a 15% denaturing polyacrylamide gel run at a constant power of 80 W. To visualize positions 6–40, the gels were run for 2.5 h, whereas longer RNA fragments (41–73) were resolved for 5.25 h. The gels were visualized using a Bio-Rad Molecular Imager FX and quantified with Bio-Rad Quantity One Software.

## ACKNOWLEDGMENTS

We thank Dr. Wai-Tak Yip for assistance with data analysis and Dr. Nils Walter for helpful discussions. This work was supported by a National Institutes of Health (NIH) predoctoral training grant (T32 GM08277) awarded to M.R.S.H. and NIH Grant AI43231.

*Received July 11, 2000; returned for revision August 16, 2000; revised manuscript received August 29, 2000*

## REFERENCES

Baker BF, Lot SS, Kringel J, Cheng-Flournoy S, Villiet P, Sasmor HM, Siwkowski AM, Chappell LL, Morrow JR. 1999. Oligonucleotide-europium complex conjugate designed to cleave the 5′ cap structure of the ICAM-1 transcript potentiates antisense activity in cells. *Nucleic Acids Res 27*:1547–1551.

Barat C, Lullien V, Schatz O, Keith G, Nugeyre MT, Grüninger-Leitch F, Barré-Sinoussi F, Le Grice SFJ, Darlix J-L. 1989. HIV-1 reverse transcriptase specifically interacts with the anticodon domain of its cognate primer tRNA. *EMBO J 8*:3279–3285.

Branum ME, Que L Jr. 1999. Double-strand DNA hydrolysis by dilanthanide complexes. *J Biol Inorg Chem 4*:593–600.

Brown RS, Dewan JC, Klug A. 1985. Crystallographic and biochemical investigation of the lead(II)-catalyzed hydrolysis of yeast phenylalanine tRNA. *Biochemistry 24*:4785–4801.

Chan B, Musier-Forsyth K. 1997. The nucleocapsid protein specifically anneals $tRNA^{Lys-3}$ onto a noncomplementary primer binding site within the HIV-1 RNA genome *in vitro*. *Proc Natl Acad Sci USA 94*:13530–13535.

Chan B, Weidemaier K, Yip W-T, Barbara PF, Musier-Forsyth K. 1999. Intra-tRNA distance measurements for nucleocapsid protein-dependent tRNA unwinding during priming of HIV reverse transcription. *Proc Natl Acad Sci USA 96*:459–464.

Ciesiolka J, Marciniec T, Krzyzosiak WJ. 1989a. Probing the environment of lanthanide binding sites in yeast $tRNA^{Phe}$ by specific metal-ion-promoted cleavage. *Eur J Biochem 182*:445–450.

Ciesiolka J, Wrzesinski J, Górnicki P, Podkowinski J, Krzyzosiak WJ. 1989b. Analysis of magnesium, europium, and lead binding sites in methionine initiator and elongator tRNAs by specific metal-ion-induced cleavages. *Eur J Biochem 186*:71–77.

Coffin JM, Hughes SH, Varmus HE. 1997. *Retroviruses*. Plainsview, New York: Cold Spring Harbor Laboratory Press.

Darlix J-L, Lapadat-Tapolsky M, de Rocquigny H, Roques BP. 1995. First glimpses at structure-function relationships of the nucleocapsid protein of retroviruses. *J Mol Biol 254*:523–537.

Das AT, Koken SEC, Essink BBO, van Wamel JLB, Berkhout B. 1994. Human immunodeficiency virus uses $tRNA^{Lys,3}$ as primer for reverse transcription in HeLa-$CD4^+$ cells. *FEBS Lett 341*:49–53.

Dorner S, Barta A. 1999. Probing ribosome structure by europium-induced RNA cleavage. *Biol Chem 380*:243–251.

Draper DE. 1985. On the coordination properties of $Eu^{3+}$ bound to tRNA. *Biophys Chem 21*:91–101.

Friederich MW, Hagerman PJ. 1997. The angle between the anticodon and aminoacyl acceptor stems of yeast $tRNA^{Phe}$ is strongly modulated by magnesium ions. *Biochemistry 36*:6090–6099.

Gast F-U, Kempe D, Spieker RL, Sänger HL. 1996. Secondary structure probing of potato spindle tuber viroid (PSTVd) and sequence comparison with other small pathogenic RNA replicons provides evidence for central non-canonical base-pairs, large A-rich loops, and a terminal branch. *J Mol Biol 262*:652–670.

Hall J, Hüsken D, Häner R. 1996. Towards artificial ribonucleases: the sequence-specific cleavage of RNA in a duplex. *Nucleic Acids Res 24*:3522–3526.

Hall J, Hüsken D, Pieles U, Moser HE, Häner R. 1994. Efficient sequence-specific cleavage of RNA using novel europium complexes conjugated to oligonucleotides. *Chem Biol 1*:185–190.

Hingerty B, Brown RS, Jack A. 1978. Further refinement of the structure of yeast $tRNA^{Phe}$. *J Mol Biol 124*:523–534.

Holbrook SR, Sussman JL, Warrant RW, Church GM, Kim S-H. 1977. RNA-ligand interactions: (I) magnesium binding sites in yeast $tRNA^{Phe}$. *Nucleic Acids Res 4*:2811–2820.

Horrocks WDeW Jr. 1993. Luminescence spectroscopy. *Methods Enzymol 226*:495–538.

Isel C, Ehresmann C, Keith G, Ehresmann B, Marquet R. 1995. Initiation of reverse transcription of HIV-1: secondary structure of the HIV-1 RNA/$tRNA_3^{Lys}$ (template/primer) complex. *J Mol Biol 247*:236–250.

Jones CR, Kearns DR. 1974. Investigation of the structure of yeast $tRNA^{Phe}$ by nuclear magnetic resonance: Paramagnetic rare earth ion probes of structure. *Proc Natl Acad Sci USA 71*:4237–4240.

Kayne MS, Cohn M. 1974. Enhancement of Tb(III) and Eu(III) fluorescence in complexes with *Escherichia coli* tRNA. *Biochemistry 13*:4159–4165.

Khan R, Chang H-O, Kaluarachchi K, Giedroc DP. 1996. Interaction of retroviral nucleocapsid proteins with transfer $tRNA^{Phe}$: A lead ribozyme and $^1H$ NMR study. *Nucleic Acids Res 24*:3568–3575.

Komiyama M. 1995. Sequence-specific and hydrolytic scission of DNA and RNA by lanthanide complex-oligo DNA hybrids. *J Biochem 118*:665–670.

Komiyama M, Matsumura K, Matsumoto Y. 1992. Unprecedentedly fast hydrolysis of the RNA dinucleoside monophosphate ApA and UpU by rare earth metal ions. *J Chem Soc Chem Commun* :640–641.

Latham JA, Cech TR. 1989. Defining the inside and outside of a catalytic RNA molecule. *Science 245*:276–282.

Magda D, Miller R, Sessler JL, Iverson BL. 1994. Site-specific hydrolysis of RNA by europium(III) texaphyrin conjugated to a synthetic oligodeoxyribonucleotide. *J Am Chem Soc 116*:7439–7440.

Maglott EJ, Deo SS, Przykorska A, Glick GD. 1998. Conformational transitions of an unmodified tRNA: Implications for RNA folding. *Biochemistry 37*:16349–16359.

Marciniec T, Ciesiolka J, Wrzesinski J, Krzyzosiak WJ. 1989. Identification of the magnesium, europium, and lead binding sites in *E. coli* and lupin $tRNA^{Phe}$ by specific metal-ion-induced cleavages. *FEBS Lett 243*:293–298.

Matsumura K, Komiyama M. 1997. Enormously fast RNA hydrolysis by lanthanide(III) ions under physiological conditions: Eminent candidates for novel tools of biotechnology. *J Biochem 122*:387–394.

Michalowski D, Wrzesinski J, Ciesiolka J, Krzyzosiak WJ. 1996. Effect of modified nucleotides on structure of yeast $tRNA^{Phe}$. Comparative studies by metal-ion-induced hydrolysis and nuclease mapping. *Biochimie 78*:131–138.

Milligan JF, Groebe DR, Witherell GW, Uhlenbeck OC. 1987. Oligoribonucleotide synthesis using T7 RNA polymerase and synthetic DNA templates. *Nucleic Acids Res 15*:8783–8798.

Misra VK, Draper DE. 2000. $Mg^{2+}$ binding to tRNA revisited: The nonlinear Poisson-Boltzmann model. *J Mol Biol 299*:813–825.

Morrow JR, Buttrey LA, Shelton VM, Berback KA. 1992. Efficient catalytic cleavage of RNA by lanthanide(III) macrocyclic complexes: Towards synthetic nucleases for *in vivo* applications. *J Am Chem Soc 114*:1903–1905.

Quigley GJ, Teeter MM, Rich A. 1978. Structural analysis of spermine and magnesium ion binding to yeast phenylalanine transfer RNA. *Proc Natl Acad Sci USA 75*:64–68.

Ramesh V, Varshney U, Rajbhandary UL. 1997. Intragenic suppression of tRNA: Evidence for crosstalk between the D and the T stems. *RNA 3*:1220–1232.

Rhim H, Park J, Morrow CD. 1991. Deletions in the $tRNA^{Lys}$ primer-binding site of human immunodeficiency virus type 1 identify essential regions for reverse transcription. *J Virol 65*:4555–4564.

Robertus JD, Ladner JE, Finch JT, Rhodes D, Brown RS, Clark BFC, Klug A. 1974. Structure of yeast phenylalanine tRNA at 3Å resolution. *Nature 250*:546–551.

Rubin JR, Sundaralingam M. 1983. Lead ion binding and RNA chain hydrolysis in phenylalanine tRNA. *J Biomol Struct Dyn 1*:639–646.

Shelton VM, Sosnick TR, Pan T. 1999. Applicability of urea in the thermodynamic analysis of secondary and tertiary RNA folding. *Biochemistry 38*:16831–16839.

Skripkin E, Isel C, Marquet R, Ehresmann B, Ehresmann C. 1996. Psoralen crosslinking between human immunodeficiency virus type 1 RNA and primer $tRNA_3^{Lys}$. *Nucleic Acids Res 24*:509–514.

Stout CD, Mizuno H, Rao ST, Swaminathan P, Rubin J, Brennan T, Sundaralingam M. 1978. Crystal and molecular structure of yeast phenylalanyl transfer RNA. Structure determination, difference Fourier refinement, molecular conformation, metal and solvent binding. *Acta Cryst B 34*:1529–1544.

Sundaralingam M, Rubin JR, Cannon JF. 1984. Nonenzymatic hydrolysis of RNA: Pb(II)-catalyzed site specific hydrolysis of transfer RNA. The role of the tertiary folding of the polynucleotide chain. *Int J Quant Chem 11*:355–366.

Tajmir-Riahi H-A, Ahmad R, Naoui M. 1993. Interaction of calf-thymus DNA with trivalent La, Eu, and Tb ions. Metal ion binding, DNA condensation and structural features. *J Biomol Struct Dyn 10*:865–877.

Takasaki BK, Chin J. 1994. Cleavage of the phosphate backbone of DNA with cerium(III) and molecular oxygen. *J Am Chem Soc 116*:1121–1122.

Wain-Hobson S, Sonigo P, Danos O, Cole S, Alizon M. 1985. Nucleotide sequence of the AIDS virus, LAV. *Cell 40*:9–17.

Walter NG, Yang N, Burke JM. 2000. Probing non-selective cation binding in the hairpin ribozyme with Tb(III). *J Mol Biol 298*:539–555.

Wolfson JM, Kearns DR. 1975. Europium as a fluorescent probe of transfer RNA structure. *Biochemistry 14*:1436–1444.